

# Bioplastic (poly-3-hydroxybutyrate)-producing *Massilia endophytica* sp. nov., isolated from *Cannabis sativa* L. 'Cheungsam'

**Doeun Jeon**

Korean Collection for Type Cultures (KCTC), Korea Research Institute of Bioscience and Biotechnology

**Lingmin Jiang**

Korean Collection for Type Cultures (KCTC), Korea Research Institute of Bioscience and Biotechnology

**Yuxin Peng**

Korean Collection for Type Cultures (KCTC), Korea Research Institute of Bioscience and Biotechnology

**Donghyun Cho**

Korean Collection for Type Cultures (KCTC), Korea Research Institute of Bioscience and Biotechnology

**Rae-dong Jeong**

Chonnam National University

**Jaecheol Jeong**

Korean Collection for Type Cultures (KCTC), Korea Research Institute of Bioscience and Biotechnology

**Jiyoung Lee** (✉ [jiyoung1@kribb.re.kr](mailto:jiyoung1@kribb.re.kr))

Korean Collection for Type Cultures (KCTC), Korea Research Institute of Bioscience and Biotechnology

**Cha Young Kim**

Korean Collection for Type Cultures (KCTC), Korea Research Institute of Bioscience and Biotechnology

---

## Article

**Keywords:** *Cannabis sativa*, FT-IR, NMR, *Massilia*, poly-3-hydroxybutyrate

**Posted Date:** May 25th, 2023

**DOI:** <https://doi.org/10.21203/rs.3.rs-2912733/v1>

**License:** © ⓘ This work is licensed under a Creative Commons Attribution 4.0 International License.

[Read Full License](#)

---

# Abstract

A rod-shaped, motile, Gram-negative bacterial strain named DM-R-R2A-13<sup>T</sup> was isolated from the plant *Cannabis sativa* L. 'Cheungsam'. The phylogenetic analysis of the 16S rRNA gene sequence revealed that strain DM-R-R2A-13<sup>T</sup> belongs to the family *Oxalobacteraceae* and is closely related to members of the genus *Massilia*, with *Massilia flava* (97.58% sequence similarity) and *Massilia armeniaca* (97.37% sequence similarity) being the closest members. The digital DNA-DNA hybridization (dDDH) values between strain DM-R-R2A-13<sup>T</sup> and *Massilia flava* CGMCC 1.10685<sup>T</sup> and *Massilia armeniaca* ZMN-3<sup>T</sup> were 22.2% and 23.3%, while the average nucleotide identity (ANI) values were 78.85% and 79.63%, respectively. The DNA G + C content was measured to be 64.6 mol%. Moreover, the bacterium was found to contain polyhydroxyalkanoate (PHA) granules based on transmission electron microscopy, indicating its potential to produce bioplastic. Genome annotation revealed the presence of PHA synthase genes (*phaC*, *phaR*, *phaP*, and *phaZ*), and the biopolymer was identified as poly-3-hydroxybutyrate (PHB) based on nuclear magnetic resonance (NMR) and Fourier transform infrared spectroscopy (FTIR) analyses. Using maltose as a carbon source, the strain produced PHB of up to 13.5% of its dry cell weight. Based on the phenotypic, chemotaxonomic, and phylogenetic characteristics, it has been determined that DM-R-R2A-13<sup>T</sup> represents a novel species belonging to the genus *Massilia*. As such, the name *Massilia endophytica* sp. nov. is proposed for this newly identified species. The type strain is DM-R-R2A-13<sup>T</sup> (= KCTC 92072<sup>T</sup> = GDMCC 1.2920<sup>T</sup>).

## Introduction

The genus *Massilia* was initially described by La Scola, who identified the species *Massilia timonae* in a blood sample from an immunocompromised patient with cerebellar lesions <sup>1</sup>. Since then, *Massilia* species have been found in a variety of environments, including soil, air, and water <sup>1-3</sup>. Kämpfer et al. suggested that all *Naxibacter* species be reclassified as *Massilia* because of their identical chemotaxonomic characteristics <sup>4</sup>. As of now, the genus *Massilia* comprises 61 species with valid and correct names. *Massilia* is a Gram-negative, rod-shaped aerobic bacteria that have relatively high DNA G + C content (63.3–66.3 mol%) <sup>5-13</sup>. The major fatty acids in this genus are summed feature 3 (C<sub>16:1</sub>ω7c and/or C<sub>16:1</sub>ω6c) and C<sub>16:0</sub>, while the major respiratory quinone is Q-8, and the major polar lipids are phosphatidylethanolamine (PE), phosphatidylglycerol (PG), and diphosphatidylglycerol (DPG) <sup>14</sup>. *Massilia* species possess diverse potential functions, such as the production of violacein <sup>15,16</sup>, degradation of benzene, toluene, ethylbenzene, and xylene (BTEX) <sup>11</sup>, solubilization of phosphate <sup>17</sup>, production of dimethyl disulfide <sup>18</sup>, adaptation to cold environments <sup>19</sup>, degradation of cellulose <sup>7</sup>, antibacterial activity <sup>8</sup>, degradation of chloroacetamide herbicide <sup>20</sup>, and accumulation of poly-3-hydroxybutyrate (PHB) <sup>21</sup>.

*Cannabis sativa* (commonly known as hemp) is among the earliest plants used by humans for food and medicine and to obtain fibers <sup>22</sup>. Hemp is a valuable source of cellulose and wood fibers and contains a

variety of phytochemicals. The outer and inner stem tissues of hemp, in particular, have garnered attention due to their potential for producing materials such as bioplastics and concrete, respectively<sup>23</sup>. As global interest in hemp research has grown, investigating endophytes in hemp has become increasingly important.

Plastic materials made from petrochemicals are currently a significant environmental issue as they are non-biodegradable<sup>24</sup>. However, PHB, a polyester synthesized by microbes that belongs to the polyhydroxyalkanoate (PHA) family, offers a promising alternative to these non-biodegradable petroleum-derived plastics<sup>25</sup>. PHB is synthesized by specific bacteria, such as *Cupriavidus necator* (formerly *Ralstonia eutropha*), using intracellular carbon and is accumulated in the cytoplasm<sup>26</sup>. PHB is biodegradable and biocompatible, and can be produced from sustainable carbon sources, making it an ideal substitute for petroleum-derived plastics like polypropylene and polyethylene<sup>27</sup>. To investigate the role of endophytic bacteria of *Cannabis sativa* L., we obtained 205 endophytic bacterial strains from the leaves and roots of the plant. One of these strains, designated DM-R-R2A-13<sup>T</sup>, was found to belong to the genus *Massilia*. The combined phenotypic and genotypic analyses indicated that DM-R-R2A-13<sup>T</sup> represents a novel species of genus *Massilia*, for which the name *Massilia endophytica* sp. nov. is proposed.

## Results and discussion

### Phylogenetic analysis using the 16S rRNA gene

To investigate endophytes in hemp, we isolated 205 endophytic bacteria from the surface-sterilized leaves and roots of the plant. Phylogenetic analysis based on the 16S rRNA gene sequence revealed that strain DM-R-R2A-13<sup>T</sup> belonged to the family *Oxalobacteraceae* and clustered with members of the genus *Massilia*. Strain DM-R-R2A-13<sup>T</sup> showed its closest relationship with *M. flava* Y9<sup>T</sup> (97.58% sequence similarity) and *M. armeniaca* ZMN-3<sup>T</sup> (97.37%). Furthermore, the sequence similarities of strain DM-R-R2A-13<sup>T</sup> with other members of the genus *Massilia* were less than 98%. In the phylogenetic trees, strain DM-R-R2A-13<sup>T</sup> was well-clustered with *M. armeniaca* (Fig. 1). The 16S rRNA gene sequence of strain DM-R-R2A-13<sup>T</sup>, which was 1,469 bp long, was deposited in the GenBank database under the accession number OL314544.

### Genomic sequencing and annotation

To construct the genome of strain DM-R-R2A-13<sup>T</sup>, we used the SMRT Link *de novo* assembler, which produced a genome size of 5,387,550 bp and an N50 value of 12,697 bp. The genome comprises a single contig and had a coverage of 135.0×. (Fig. S1). The whole-genome sequence was deposited in GenBank (accession number: CP088952). The DNA G + C content of strain DM-R-R2A-13<sup>T</sup> is 64.6%, which falls within the range of *Massilia* species. The annotation of the NCBI Prokaryotic Genome Annotation Pipeline (PGAP) identified a total of 4,800 protein-coding genes and 94 RNA genes in the genome, including 6 5S

rRNA genes, 6 16S rRNA genes, 6 23S rRNA genes, 72 tRNA genes, and 4 ncRNA genes. Cluster Orthologous Group (COG) annotation showed that a large proportion of the assigned COGs were classified as unknown (30.6% of total assigned COGs), while signal transduction mechanisms (7.2% of the total assigned COGs) and transcription (6.5% of the total assigned COGs) were among the most represented categories (Fig. S2).

The dDDH and ANI values between strain DM-R-R2A-13<sup>T</sup> and *Massilia flava* CGMCC 1.10685<sup>T</sup> (VLKW01000000), *Massilia armeniaca* ZMN-3<sup>T</sup> (CP028324), and *Massilia timonae* CCUG 45783<sup>T</sup> (AGZI01000000) were 22.2%, 23.3%, and 20.6%, and 78.85%, 79.63%, and 75.83%, respectively. The whole-genome phylogenetic tree, which was constructed based on the concatenated 92 core genes, also supported the position of strain DM-R-R2A-13<sup>T</sup> within the genus *Massilia* (Fig. 2).

## Phenotypic and chemotaxonomic characterization

Strain DM-R-R2A-13<sup>T</sup> is a Gram-negative, rod-shaped aerobic bacteria that has light pink colonies and possesses flagella for motility (Fig. S3). The optimal conditions for cell growth were 30–37°C and pH 6.0–7.5. It was noted that the strain grew well in the absence of NaCl. Transmission-electron microscopy (TEM) analysis indicated several white particles such as PHB granules with high refraction (Fig. 3). Notably, the strain had phenotypic characteristics that helped to distinguish it from its closely related species (Table 1), including the assimilation of N-acetyl-glucosamine. Furthermore, the strain was sensitive to the antibiotics kanamycin, tetracycline, and nalidixic acid.

Table 1

**Distinguishing characteristics between strain DM-R-R2A-13<sup>T</sup> and its closely related species in the genus *Massilia*.** Strains: 1, DM-R-R2A-13<sup>T</sup>; 2, *M. flava* KCTC 23535<sup>T</sup>; 3, *M. armeniaca* DSM 104676<sup>T</sup>; 4, *M. timonae* DSM 16850<sup>T</sup>; +, positive; -, negative; w, weakly positive; ND, no data available.

Characteristics	1	2	3	4
Isolation source	<i>Cannabis sativa</i>	Soil <sup>a</sup>	Desert soil <sup>b</sup>	Blood of an Immunocompromised Patient <sup>c</sup>
Motility	Motile	ND	Motile <sup>b</sup>	Motile <sup>c</sup>
Colony color	Light pink	Yellow <sup>a</sup>	Apricot <sup>b</sup>	Straw <sup>c</sup>
Oxidase/catalase activity	+/+	+/+ <sup>a</sup>	-/+ <sup>b</sup>	+/+ <sup>c</sup>
Enzyme activity (API ZYM)				
crystine arylamidase	+	+	-	+
Trypsin	-	-	-	-
α-chymotrypsin	w	-	-	w
α-galactosidase	-	+	+	-
β-galactosidase	+	+	-	-
α-glucosidase	+	+	+	-
β-glucosidase	+	-	-	+
Assimilation activity (API 20NE)				
D-glucose	-	-	-	-
L-arabinose	+	-	-	+
N-acetyl-D-galactosamine	+	-	-	-
D-maltose	+	-	-	+
Potassium gluconate	-	-	-	w
malic acid	w	-	-	+
trisodium citrate	-	-	-	+
Antibiotic sensitivity				
Kannamycin	+	+	+	+

<sup>a</sup>Data from Wang et al.[12], ; <sup>b</sup>Data from Ren et al.[10]; <sup>c</sup>Data from La Scola et al.[1].

Characteristics	1	2	3	4
Tetracyclin	+	+	+	+
Chloramphenicol	-	-	+	+
Nalidixic acid	+	-	+	+

<sup>a</sup>Data from Wang et al.[12], ; <sup>b</sup>Data from Ren et al.[10]; <sup>c</sup>Data from La Scola et al.[1].

The polar lipids in the strain were PE, PG and DPG (which are common in closely related species in the genus *Massilia*), one unidentified phospholipid (PL), and four unidentified aminolipids (AL) (Fig. S4). The dominant fatty acids observed in the strain were C<sub>16:0</sub> and summed feature 3 (C<sub>16:1</sub>ω7c and/or C<sub>16:1</sub>ω6c) as shown in Table 2. Furthermore, the respiratory quinone analysis revealed the presence of ubiquinone Q-8, a characteristic quinone found in the genus *Massilia*. Based on these findings, it is proposed that strain DM-R-R2A-13<sup>T</sup> be classified as a novel species of the genus *Massilia*, with the name *Massilia endophytica* sp. nov.

Table 2

**Cellular fatty acid compositions (> 1%) of strain DM-R-R2A-13<sup>T</sup> and its closely related species in the genus *Massilia*. Strains: 1, DM-R-R2A-13<sup>T</sup>; 2, *M. flava* KCTC 23535<sup>T</sup>; 3, *M. armeniaca* DSM 104676<sup>T</sup>; 4, *M. timonae* DSM 16850<sup>T</sup>; -, not detected. Major components (> 10%) are shown in bold. All data were obtained from the present study.**

Fatty acid	1	2	3	4
C <sub>10:0</sub>	0.58	-	-	0.47
C <sub>10:0</sub> 3-OH	4.76	2.41	4.92	4.46
C <sub>12:0</sub>	4.33	3.9	4.15	4.36
C <sub>12:0</sub> 2-OH	2.8	-	-	2.02
C <sub>12:0</sub> 3-OH	-	3.32	-	-
C <sub>14:1</sub> ω5c	0.6	0.74	1.34	0.67
C <sub>14:0</sub>	0.69	1.01	1.31	0.45
C <sub>14:0</sub> 2-OH	-	2.54	3.06	-
iso-C <sub>16:0</sub>	0.32	-	-	-
C <sub>16:0</sub>	<b>33.71</b>	<b>30.94</b>	<b>27.47</b>	<b>34.24</b>
C <sub>17:1</sub> ω5c	0.62	1.02	-	-
C <sub>17:0</sub> cyclo	4.61	3.57	-	0.77
summed feature 3*	<b>39.9</b>	<b>39.77</b>	<b>46.79</b>	<b>44.48</b>
summed feature 8*	7.09	<b>10.77</b>	<b>10.96</b>	8.08
* Summed features are groups of one or two fatty acids that cannot be separated by GLC with the MIDI Sherlock version 4.5 system. Summed feature 3 contained C <sub>16:1</sub> ω7c and/or C <sub>16:1</sub> ω6c and summed feature 8 contained C <sub>18:1</sub> ω7c. The database used was TSBA6.				

## PHB biosynthetic pathway

Since the TEM micrographs showed bacterial cells containing PHB granules in their cytoplasm, we performed a comprehensive analysis, including BlastKOALA analysis and NCBI PGAP analysis on the complete genome. The homopolymer PHB is one of the most extensively investigated compounds among the polyhydroxyalkanoates (PHA) family<sup>41</sup>. The BlastKOALA analysis showed that the PHB biosynthesis pathway of DM-R-R2A-13<sup>T</sup> belongs to butanoate metabolism. This PHB biosynthesis process begins with the condensation of two acetyl-CoA units (obtained after fatty acid degradation) by acetyl-CoA C-acetyltransferase (atoB) to form acetoacetyl-CoA. This compound is then reduced by PHA

synthase (phaC) to yield PHA, specifically (R)-3-hydroxyl-butanoyl-CoA, which is ultimately converted into PHB<sup>42</sup> (Fig. 4A).

## PHA-associated gene cluster

The enzyme responsible for PHB synthesis is phaC, which polymerizes monomers into PHA polymer. PhaC's substrate specificity determines the type of monomers that are incorporated into the PHA chain. There are four classes of PHA synthase, each with unique characteristics<sup>43</sup>. Class I and II PHA synthases are composed solely of PhaC. Class I PHA synthases, such as those found in *Cupriavidus necator* (formerly *Ralstonia eutropha*), exhibit a preference for CoA thioesters of (R)-3-hydroxy fatty acids that have 3–5 carbon atoms. On the other hand, class II PHA synthases, as seen in *Pseudomonas aeruginosa*, tend to favor CoA thioesters of (R)-3-hydroxy fatty acids that have 6–14 carbon atoms<sup>44–46</sup>. Class III PHA synthases, found in *Allochromatium vinosum*, are composed of two distinct enzymes, PhaC and PhaE, and they prefer CoA thioesters of (R)-3-hydroxy fatty acids with 3–5 carbon atoms<sup>47,48</sup>. In class IV PHA synthases, such as those found in *Bacillus megaterium*, there are two distinct enzymes, PhaC and PhaR, where PhaR substitutes PhaE in class III PHA synthases. NCBI-based genome annotation of strain DM-R-R2A-13<sup>T</sup> identified multiple genes associated with PHA metabolism, including PhaC, PhaR, PhaZ, and PhaP. It is clear that the PhaC gene in DM-R-R2A-13<sup>T</sup> belongs to Class I (Fig. 4B). We utilized Cluster Omega multiple sequence alignment to compare the sequence similarity of PhaC and PhaR genes with those of strains representing each class. The results indicated high similarity to PhaC of *C. necator*, which belongs to class 1 (Table S1).

## Polymer analysis

FT-IR spectrum of PHB extracted from DM-R-R2A-13<sup>T</sup> exhibited several absorption peaks. These include an OH group peak at 2930cm<sup>-1</sup>, C = O stretching of an ester group peaks at 1720cm<sup>-1</sup>, aliphatic –CH<sub>2</sub> and –CH<sub>3</sub> group peaks at 1453cm<sup>-1</sup> and 1379cm<sup>-1</sup>, respectively, and –CH group peaks at 1276cm<sup>-1</sup> (Fig. 5A). The absorption peaks of the extracted PHB were similar to those of commercial PHB, as shown in Fig. 5B.

A <sup>1</sup>H NMR analysis was utilized to analyze the chemical structure of PHB synthesized by the strain DM-R-R2A-13<sup>T</sup>. The <sup>1</sup>H NMR spectrum had peaks at 1.26–1.28 ppm (–CH<sub>3</sub>), 2.45–2.62 ppm (–CH<sub>2</sub>), and 5.24–5.28 ppm (–CH) (Fig. 5C), confirming the chemical structure of PHB<sup>49</sup>. Additionally, the <sup>13</sup>C NMR spectrum was analyzed to confirm the extracted PHB's structure (Fig. 5D). The peaks corresponded to various carbon atoms within the PHB structure, including peaks at 169.15 ppm (C = O), 67.61 ppm (–CH), 40.79 ppm (–CH<sub>2</sub>), and 19.76 ppm (–CH<sub>3</sub>).

## Effect of carbon source on PHB production

The study examined whether the PHB production of DM-R-R2A-13<sup>T</sup> was influenced by different carbon sources under optimal conditions. Figure 6 showed that maltose (13.5% per cdw) resulted in the highest



PHB content, followed by lactose (10.1% per cdw) and starch (2.9% per cdw).

## Conclusion

In this study, we investigated strain DM-R-R2A-13<sup>T</sup>, which was obtained from the plant *Cannabis sativa* L. 'Cheungsam'. Based on a polyphasic taxonomic approach that integrates phenotypic, chemotaxonomic, and phylogenomic characteristics, this strain exhibiting distinct phylogenetic lineages has been designated as novel species. Consequently, it has been assigned the name *Massilia endophyticus* sp. nov. We observed that the bacterium contained granules of PHA, indicating its potential for bioplastic production. The analysis of the genome revealed the presence of PHA synthase genes (*phaC*, *phaR*, *phaP*, and *phaZ*), further supporting its capability for biopolymer synthesis. Through NMR and FT-IR analyses, the biopolymer was identified as poly-3-hydroxybutyrate (PHB). Notably, when maltose was utilized as the carbon source, the strain exhibited the highest PHB production rate of up to 13.5% of its dry cell weight.

### Description of *Massilia endophytica* sp. nov.

*Massilia endophyticus* (en.do.phy'ti.ca. Gr. pref. *endo-*, within; Gr. neut. n. *phyton* plant; L. fem. suff. *-ica*, adjectival suffix used with the sense of belonging to; N.L. fem. adj. *endophytica* within plants; *endophytic* pertaining to the original isolation from plant tissues).

Cells are Gram-negative, rod-shaped, aerobic, and motile. The colonies on R2A agar plates are circular, convex, and light pink in color, with a size of 1.5–2.0 μm after 2 days of incubation at 30°C. The strain grows optimally at temperatures of 30–37°C (it can grow at 15–40°C) and pH values ranging from 6.0–7.5 (it can grow at pH 5.5–9.0), with optimal growth in the absence of NaCl. The strain showed sensitivity to kanamycin, tetracycline, and nalidixic acid in the antibiotic sensitivity tests. Catalase and oxidase are positive. Positive results were observed for alkaline phosphatase, esterase (C4), esterase lipase (C8), leucine arylamidase, valine arylamidase, cystine arylamidase, acid phosphatase, naphthol-AS-BI-phosphohydrolase, and β-glucosidase. Lipase (C14), trypsin, and α-chymotrypsin showed weak activity. Conversely, α-galactosidase, β-galactosidase, β-glucuronidase, α-glucosidase, N-acetyl-β-glucosaminidase, α-mannosidase, and α-fucosidase were negative according to the API ZYM strips. The API 20 NE results showed positive assimilation for potassium nitrate, esculin ferric citrate, L-arabinose, D-mannose, N-acetyl-glucosamine, and D-maltose. However, the assimilation of malic acid was weak. The DNA G + C content of the type strain is 64.6%. The dominant fatty acids are C<sub>16:0</sub> and summed feature 3 (C<sub>16:1</sub>ω7c and/or C<sub>16:1</sub>ω6c). The major polar lipids are phosphatidylethanolamine (PE), phosphatidylglycerol (PG), and diphosphatidylglycerol (DPG). The predominant ubiquinone is Q-8.

The type strain DM-R-R2A-13<sup>T</sup> (= KCTC 92072<sup>T</sup>, GDMCC 1.2920<sup>T</sup>) was isolated from *Cannabis sativa* L. from Andong, Republic of Korea. The GenBank accession numbers for the 16S rRNA and the whole genome sequence of strain DM-R-R2A-13<sup>T</sup> are OL314544 and CP088952, respectively.

## Materials and methods

### Sample collection and bacterial isolation

The strain DM-R-R2A-13<sup>T</sup> was obtained from a sample of *Cannabis sativa* in Andong, Republic of Korea. To isolate the strain, leaf samples (5.3 g) and root samples (6.3 g) were subjected to surface-sterilization using 1% sodium hypochlorite for 20 min followed by 70% ethanol for 10 s, and then rinsed with sterile water. The sterilized samples were ground with 25 mL distilled water and spread onto plates containing Reasoner's 2A (R2A) medium after serial dilution. The plates were incubated at 25°C for 3 days, after which single colonies were isolated by transferring them onto new plates containing R2A medium and re-incubating. The strains were deposited at two culture collections: the Korean Collection for Type Cultures (KCTC) and the Guangdong Microbial Culture Collection Center (GDMCC), with accession numbers KCTC 92072<sup>T</sup> and GDMCC 1.2920<sup>T</sup>, respectively.

### Phylogenetic analysis

To amplify the 16S rRNA gene of strain DM-R-R2A-13<sup>T</sup>, we used universal primers 518F and 800R as previously described<sup>28</sup>. The species with the closest match to the DM-R-R2A-13<sup>T</sup> 16S rRNA gene sequence was obtained from the EzBioCloud server (<http://www.ezbiocloud.net>)<sup>29</sup>. Multiple sequence alignment was performed using all valid published members of the *Oxalobacteraceae* family with BioEdit (v.7.2.5). The nearly complete 16S rRNA gene sequence was submitted to the GenBank database (GenBank accession number, OL314544). To generate a phylogenetic tree, we employed the neighbor-joining (NJ), minimum evolution (ME), and maximum likelihood (ML) methods in MEGA X with 1,000 bootstrap replications<sup>30</sup>. *Oxalobacter formigenes* U49757.2<sup>T</sup> was used as the outgroup.

### Genomic sequencing and annotation

Genomic DNA was extracted for whole-genome sequencing using the protocol developed by Wilson et al.<sup>29</sup>. The sequencing was carried out at Macrogen, Inc. (Daejeon, Republic of Korea) using a PacBio Sequel/Sequel 2 system and an Illumina platform. The resulting data were assembled using a SMRT Link (v.8) *de novo* assembler. To determine the digital DNA–DNA hybridization (dDDH) and average nucleotide identity (ANI) values between DM-R-R2A-13<sup>T</sup> and closely related strains, we employed the Genome-to-Genome Distance Calculation (GGDC) web server (<http://ggdc.dsmz.de/>) and EzBioCloud ANI calculator ([www.ezbiocloud.net/tools/ani](http://www.ezbiocloud.net/tools/ani))<sup>31,32</sup>, utilizing the BLAST method. Metabolic features and pathways were determined by utilizing BlastKOALA, a tool that utilizes the Kyoto Encyclopedia of Genes and Genomes (KEGG) orthology system<sup>33</sup>. Genome annotation was also performed using the National Center for Biotechnology Information (NCBI) Prokaryotic Genome Annotation Pipeline<sup>34</sup>. A whole-genome phylogenetic tree was created using the up-to-date bacterial core gene set and pipeline (UBCG) as described by Na et al.<sup>35</sup>. *Oxalobacter formigenes* U49757.2<sup>T</sup> was used as the outgroup.

### Phenotypic and chemotaxonomic traits

Strain DM-R-R2A-13<sup>T</sup> was cultivated on various growth media, including Luria–Bertani agar (LBA, Difco), marine agar 2216 (MA, Difco), malt extract agar (MEA, Difco), potato dextrose agar (PDA, Difco), Reasoner’s 2A agar (R2A, MB Cell), and tryptic soy agar (TSA, Difco). Growth in R2A broth was measured at various temperatures (4, 10, 15, 20, 25, 30, 35, 37, 40, 45, 50, and 55°C), pH values (pH 3.0–12.0, at intervals of 0.5 pH unit), and NaCl concentrations (0, 0.05, 0.1, 0.15, 0.2, 0.5, and 1.0%; w/v) after 2 days of incubation. Gram staining was conducted using a Gram Stain Solution kit (Difco). Catalase activity was tested using 1.0% tetramethyl-p-phenyldiamine (Oxidase Reagent Kit, bioMérieux). Anaerobic growth was determined by incubating the strain on R2A medium in an anaerobic chamber with an 86% N<sub>2</sub>, 7% CO<sub>2</sub>, and 7% H<sub>2</sub> atmosphere at 30°C for 14 days.

Cell motility was evaluated using R2A medium containing 0.4% agar, and the presence of flagella was assessed by scanning electron microscopy (SEM); the cells were fixed with 2% glutaraldehyde and 2% paraformaldehyde in 50 mM cacodylate buffer (pH 7.4) for 1 h at 4°C. Antibiotic sensitivity was determined using antibiotic discs (BD BBL™) containing one of the following antibiotics: (µg/disc): chloramphenicol (30), kanamycin (30), nalidixic acid (30), nitrofurantoin (300), tetracycline (30), and penicillin (10 U) on R2A medium. Enzyme activity and assimilation activity were determined using API 20 NE (bioMérieux) and API ZYM (bioMérieux), respectively.

To determine the fatty acid content, strain DM-R-R2A-13<sup>T</sup> and reference strains (KCTC 23585<sup>T</sup>, DSM 104676<sup>T</sup>, and DSM 16850<sup>T</sup>) were cultivated for 2 days on R2A. Cells harvested from the culture were subjected to fatty acid methyl ester extraction following the standard MIDI instructions (Sherlock Microbial Identification System v.6.0), and the resulting samples were analyzed using gas chromatography (model 6890N; Agilent) with the Microbial Identification software package (TSBA database v.6.0)<sup>36</sup>. Freeze-dried cells (100 mg) were employed to extract isoprenoid quinones using a methanol/isopropyl ether (3:1, v/v) mixture, followed by thin-layer chromatography analysis, as previously described by Colins et al.<sup>37</sup>. Polar lipids were extracted from freeze-dried cells (100 mg) using a chloroform/methanol mixture (2:1, v/v). The separation of polar lipids was achieved by two-dimensional thin-layer chromatography (silica gel, 20 × 20 cm; Merck) followed by spraying with phosphomolybdic acid to identify polar lipids<sup>38</sup>.

## Transmission electron microscopy (TEM)

The samples were fixed with a solution containing 2% glutaraldehyde and 2% paraformaldehyde in 50 mM cacodylate buffer (pH 7.4) for 1 h at 4°C, followed by post-fixation with 2% osmium tetroxide and 3% potassium hexacyanoferrate for 40 minutes. Subsequently, the samples were dehydrated in a graded series of ethanol, with each dilution lasting for 10 minutes, the samples were immersed in a mixture of 100% ethanol and LR white resin (in ratios of 2:1, 1:1, or 1:2) for 10 minutes, and then transferred to pure LR white resin for an additional 15 min. The samples were transferred to a dry capsule or mold, which was filled with embedding resin. The resin was cured in a 60°C oven for 24 h. The samples were then subjected to ultra-thin sectioning (80 nm), placed on a copper grid, stained with uranyl acetate and lead

citrate, and viewed using TEM (JEM-2100F, JEOL) at an accelerating voltage of 200 kV at the Korea Basic Science Institute (Chuncheon, Republic of Korea).

## Extraction and purification of PHB

The extraction and purification of PHB followed the experimental method detailed by Trakunke et al.<sup>39</sup>. For the extraction of PHB, freeze-dried cells (1g) were dissolved in 100 mL of chloroform and allowed to stand at room temperature for 4 days. Afterward, the solutions were filtered using ADVANTEC filter paper (90 mm) to eliminate any cellular debris and obtain a purified solution. Subsequently, the filtrate was slowly added dropwise to 100 mL of cold-methanol (Honeywell, USA). The resulting purified polymer was air-dried for 3 days and collected for Fourier transform infrared (FT-IR) spectroscopy and nuclear magnetic resonance (NMR) analysis to confirm its chemical structure as polyhydroxybutyrate (PHB).

## FT-IR spectroscopy

FT-IR spectroscopy was conducted using a Bruker Lumos II FT-IR microscope at Koptri Inc. (Seoul, Republic of Korea). The samples were scanned within a wavenumber range of 4,000–400  $\text{cm}^{-1}$  at a resolution of 4  $\text{cm}^{-1}$ , with a total of 32 scans per sample.

## NMR analysis

Both  $^1\text{H}$  NMR and  $^{13}\text{C}$  NMR spectra were obtained using a Bruker Avance™ HD 600 MHz at Koptri Inc. (Seoul, Republic of Korea). The bacterial-isolated PHB samples, as well as the standard PHB (Sigma-Aldrich, USA), were dissolved in chloroform. Tetramethylsilane (TMS) signals were used as reference standards for the chemical shifts observed in the  $^1\text{H}$  and  $^{13}\text{C}$  spectra.

## Effect of carbon source on PHB production

PHB production by strain DM-R-R2A-13<sup>T</sup> was explored in a 250-mL Erlenmeyer flask containing 100 mL R2A medium after the removal of existing carbon sources (casamino acid, 0.5 g/L; yeast extract, 0.5 g/L; proteose peptone, 0.5 g/L; dipotassium phosphate, 0.3 g/L; magnesium sulfate, 0.05 g/L) and the addition of a new carbon source (glucose, starch, maltose, fructose, sucrose, or lactose); 1.3 g/L replacement carbon source was used, which is the amount of the existing carbon sources in the R2A medium. The flasks were incubated in a shaker at 150 rpm and 30°C for 48 h. Cells were obtained after centrifuging the culture at 8,000 rpm for 15 min, and the samples were freeze-dried for at least 24 h. Lyophilization was deemed complete when the cell pellets were dry. All experiments were performed in triplicate.

## Gas chromatography (GC)

To quantify the PHB, GC was used with a DB-23 capillary column (60 m × 250  $\mu\text{m}$  × 0.25  $\mu\text{m}$ ). The PHB was converted to 3-hydroxybutyryl methyl ester (3-HBME), a stable monomer, in the GC column using the acidic methanolysis method. Freeze-dried cells (10 mg) were mixed with 1 mL chloroform and 1 mL methanol containing 15% (v/v)  $\text{H}_2\text{SO}_4$  and incubated for 2.5 h at 100°C. After cooling the samples on ice

for 5 min, 1 mL deionized water and 1 mL chloroform containing 0.2% (v/v) methyl benzoate as an internal standard were added. The mixture was vortexed and the organic (bottom) phase containing methylesters was used for PHB analysis. Commercial PHB (Sigma-Aldrich) was used as the reference standard. The GC configuration parameters were set as follows: injection volume, 1  $\mu$ L; split ratio, 1:25; injection temperature, 250°C; column oven temperature, 80°C for 2 min; and temperature ramp, 10°C/min<sup>-1</sup> and 245°C for 1 min. The detection was performed using a flame ionization detector at 275°C.

## Quantification of PHB

The weight of PHB was estimated using a standard curve constructed based on commercial PHB (Sigma-Aldrich) at various concentrations (2, 4, 6, and 8 mg) following the formula used by Jannina et al.<sup>40</sup>. The normalized area of 3-HBME peaks was calculated using the following formula:

$$\text{Normalized area} = \frac{\text{Area of 3HBME} * \text{Area of external standard}}{\text{Area of internal standard}}$$

The weight of PHB in a sample with various carbon sources was calculated using the following formula:

$$\text{Weight of PHB in sample} = \frac{\text{Normalized area of sample} - b}{a}$$

a is a standard curve's slope and b is a standard curve's y-intercept.

The percentage of PHB per cell dry weight (cdw) was calculated using the following formula:

$$\text{PHB content (\% per cdw)} = \text{Weight of PHB in sample} * \frac{100}{\text{weighed cells}}$$

## Statistical analysis

The data were analyzed using one-way analysis of variance (ANOVA) in GraphPad Prism v.9, and the results are presented as mean  $\pm$  standard deviation. Error bars indicate standard error (n = 3). A significant level of p-value  $\leq$  0.05 was used to determine statistical significance.

## Declarations

### Acknowledgments

We thank Dr. Gwang Joong Kim at the Korea Basic Science Institute (KBSI, Chuncheon Center) for the SEM and TEM images. This work was supported by Korea Institute of Planning and Evaluation for Technology in Food, Agriculture, and Forestry (IPET) through the Agricultural Machinery/Equipment Localization Technology Development Program, funded by the Ministry of Agriculture, Food and Rural Affairs (MAFRA) (321057051HD020), and by the KRIBB research initiative program.

### Author contributions

JL and JJ: designed the research and supervised the project, modified the manuscript. DJ and LJ: performed the experiment, data analyzed and wrote the original draft, and modified the manuscript. YP, DC, RJ and CYK: edited the manuscript. All authors read and approved the manuscript.

### Ethics approval

Experimental research and field studies on plants, including the collection of plant material, complying with relevant institutional, national, and international guidelines and legislation.

### Data availability

Strain DM-R-R2A-13<sup>T</sup> can be obtained from two culture collections, the Korean Collection for Type Cultures (KCTC 92072<sup>T</sup>) and the Guangdong Microbial Culture Collection Center (GDMCC 1.2920<sup>T</sup>). The 16S rRNA gene sequence of strain DM-R-R2A-13<sup>T</sup> is available under GenBank accession number OL314544, while the whole-genome sequence is CP088952. The associated BioSample and BioProject accession numbers are SAMN23170019 and PRJNA678113, respectively. The taxonomy ID for strain DM-R-R2A-13<sup>T</sup> is 2899220.

### Competing interest

The author(s) declare no competing interests.

### Additional information

The followings are supplementary data to this article can be found online at:

Supplementary Figure S1-S4 and Table S1.

## References

1. La Scola, B., Birtles, R. J., Mallet, M. N. & Raoult, D. *Massilia timonae* gen. nov., sp. nov., isolated from blood of an immunocompromised patient with cerebellar lesions. *J. Clin. Microbiol.* **36**, 2847-2852, doi:10.1128/JCM.36.10.2847-2852.1998 (1998).
2. Luo, X. *et al.* *Massilia lurida* sp. nov., isolated from soil. *Int. J. Syst. Evol. Microbiol.* **63**, 2118-2123, doi:10.1099/ijs.0.047068-0 (2013).
3. Weon, H. Y. *et al.* *Massilia niabensis* sp. nov. and *Massilia niastensis* sp. nov., isolated from air samples. *Int. J. Syst. Evol. Microbiol.* **59**, 1656-1660, doi:10.1099/ijs.0.006908-0 (2009).
4. Kämpfer, P., Lodders, N., Martin, K. & Falsen, E. Revision of the genus *Massilia* La Scola *et al.* 2000, with an emended description of the genus and inclusion of all species of the genus *Naxibacter* as new combinations, and proposal of *Massilia consociata* sp. nov. *Int. J. Syst. Evol. Microbiol.* **61**, 1528-1533, doi:10.1099/ijs.0.025585-0 (2011).

5. Baek, J. H. *et al.* *Massilia soli* sp. nov., isolated from soil. *Int. J. Syst. Evol. Microbiol.* **72**, 005227, doi:10.1099/ijsem.0.005227 (2022).
6. Dahal, R. H., Chaudhary, D. K. & Kim, J. Genome insight and description of antibiotic producing *Massilia antibiotica* sp. nov., isolated from oil-contaminated soil. *Sci. Rep.* **11**, 1-11, doi:10.1038/s41598-021-86232-z (2021).
7. Du, C. *et al.* *Massilia cellulositytica* sp. nov., a novel cellulose-degrading bacterium isolated from rhizosphere soil of rice (*Oryza sativa* L.) and its whole genome analysis. *Antonie Van Leeuwenhoek* **114**, 1529-1540, doi:10.1007/s10482-021-01618-3 (2021).
8. Li, C. *et al.* *Massilia rhizosphaerae* sp. nov., a rice-associated rhizobacterium with antibacterial activity against *Ralstonia solanacearum*. *Int. J. Syst. Evol. Microbiol.* **71**, 005009, doi:10.1099/ijsem.0.005009 (2021).
9. Peta, V., Raths, R. & Bucking, H. *Massilia horti* sp. nov. and *Noviherbaspirillum arenae* sp. nov., two novel soil bacteria of the *Oxalobacteraceae*. *Int. J. Syst. Evol. Microbiol.* **71**, 004765, doi:10.1099/ijsem.0.004765 (2021).
10. Ren, M. *et al.* *Massilia armeniaca* sp. nov., isolated from desert soil. *Int. J. Syst. Evol. Microbiol.* **68**, 2319-2324, doi:10.1099/ijsem.0.002836 (2018).
11. Son, J., Lee, H., Kim, M., Kim, D. U. & Ka, J. O. *Massilia aromaticivorans* sp. nov., a BTEX Degrading Bacterium Isolated from Arctic Soil. *Curr. Microbiol.* **78**, 2143-2150, doi:10.1007/s00284-021-02379-y (2021).
12. Wang, J. *et al.* *Massilia flava* sp. nov., isolated from soil. *Int. J. Syst. Evol. Microbiol.* **62**, 580-585, doi:10.1099/ijse.0.031344-0 (2012).
13. Yang, R. *et al.* *Massilia puerhi* sp. nov., isolated from soil of Pu-erh tea cellar. *Int. J. Syst. Evol. Microbiol.* **71**, 004992, doi:10.1099/ijsem.0.004992 (2021).
14. Holochova, P. *et al.* Description of *Massilia rubra* sp. nov., *Massilia aquatica* sp. nov., *Massilia mucilaginoso* sp. nov., *Massilia frigida* sp. nov., and one *Massilia* genomospecies isolated from Antarctic streams, lakes and regoliths. *Syst. Appl. Microbiol.* **43**, 126112, doi:10.1016/j.syapm.2020.126112 (2020).
15. Agematu, H., Suzuki, K. & Tsuya, H. *Massilia* sp. BS-1, a novel violacein-producing bacterium isolated from soil. *Biosci. Biotechnol. Biochem.* **75**, 2008-2010, doi:10.1271/bbb.100729 (2011).
16. Myeong, N. R., Seong, H. J., Kim, H. J. & Sul, W. J. Complete genome sequence of antibiotic and anticancer agent violacein producing *Massilia* sp. strain NR 4-1. *J. Biotechnol.* **223**, 36-37, doi:10.1016/j.jbiotec.2016.02.027 (2016).
17. Zheng, B. X., Bi, Q. F., Hao, X. L., Zhou, G. W. & Yang, X. R. *Massilia phosphatilytica* sp. nov., a phosphate solubilizing bacteria isolated from a long-term fertilized soil. *Int. J. Syst. Evol. Microbiol.* **67**, 2514-2519, doi:10.1099/ijsem.0.001916 (2017).
18. Feng, G. D., Yang, S. Z., Li, H. P. & Zhu, H. H. *Massilia putida* sp. nov., a dimethyl disulfide-producing bacterium isolated from wolfram mine tailing. *Int. J. Syst. Evol. Microbiol.* **66**, 50-55, doi:10.1099/ijsem.0.000670 (2016).

19. Dahal, R. H., Chaudhary, D. K., Kim, D. U. & Kim, J. Cold-shock gene *cspC* in the genome of *Massilia polaris* sp. nov. revealed cold-adaptation. *Antonie Van Leeuwenhoek* **114**, 1275-1284, doi:10.1007/s10482-021-01600-z (2021).
20. Lee, H., Kim, D. U., Park, S., Yoon, J. H. & Ka, J. O. *Massilia chloroacetimidivorans* sp. nov., a chloroacetamide herbicide-degrading bacterium isolated from soil. *Antonie Van Leeuwenhoek* **110**, 751-758, doi:10.1007/s10482-017-0845-3 (2017).
21. Rodriguez-Diaz, M. *et al.* *Massilia umbonata* sp. nov., able to accumulate poly-beta-hydroxybutyrate, isolated from a sewage sludge compost-soil microcosm. *Int. J. Syst. Evol. Microbiol.* **64**, 131-137, doi:10.1099/ijms.0.049874-0 (2014).
22. Mechoulam, R. The pharmacohistory of *Cannabis sativa*. *Cannabinoids as therapeutic agents*, 1-20, doi:10.1201/9780429260667-1 (2019).
23. Andre, C. M., Hausman, J. F. & Guerriero, G. *Cannabis sativa*: The Plant of the Thousand and One Molecules. *Front. Plant. Sci.* **7**, 19, doi:10.3389/fpls.2016.00019 (2016).
24. Getachew, A. & Woldesenbet, F. Production of biodegradable plastic by polyhydroxybutyrate (PHB) accumulating bacteria using low cost agricultural waste material. *BMC Res Notes* **9**, 509, doi:10.1186/s13104-016-2321-y (2016).
25. McAdam, B., Brennan Fournet, M., McDonald, P. & Mojicevic, M. Production of Polyhydroxybutyrate (PHB) and Factors Impacting Its Chemical and Mechanical Characteristics. *Polymers (Basel)* **12**, doi:10.3390/polym12122908 (2020).
26. Lee, K.-M., Gimore, D. & Huss, M. Fungal degradation of the bioplastic PHB (Poly-3-hydroxy-butyric acid). *J. Polym. Environ.* **13**, 213-219, doi:10.1007/s10924-006-0013-8 (2005).
27. Naranjo, J. M., Cardona, C. A. & Higuera, J. C. Use of residual banana for polyhydroxybutyrate (PHB) production: case of study in an integrated biorefinery. *Waste Manage.* **34**, 2634-2640, doi:10.1016/j.wasman.2014.09.007 (2014).
28. Lane, D. 16S/23S rRNA sequencing. *Nucleic acid techniques in bacterial systematics* (1991).
29. Yoon, S. H. *et al.* Introducing EzBioCloud: a taxonomically united database of 16S rRNA gene sequences and whole-genome assemblies. *Int. J. Syst. Evol. Microbiol.* **67**, 1613-1617, doi:10.1099/ijsem.0.001755 (2017).
30. Kumar, S., Stecher, G., Li, M., Nnyaz, C. & Tamura, K. MEGA X: Molecular Evolutionary Genetics Analysis across Computing Platforms. *Mol. Biol. Evol.* **35**, 1547-1549, doi:10.1093/molbev/msy096 (2018).
31. Meier-Kolthoff, J. P., Auch, A. F., Klenk, H. P. & Goker, M. Genome sequence-based species delimitation with confidence intervals and improved distance functions. *BMC Bioinform.* **14**, 60, doi:10.1186/1471-2105-14-60 (2013).
32. Yoon, S. H., Ha, S. M., Lim, J., Kwon, S. & Chun, J. A large-scale evaluation of algorithms to calculate average nucleotide identity. *Antonie Van Leeuwenhoek* **110**, 1281-1286, doi:10.1007/s10482-017-0844-4 (2017).



33. Kanehisa, M., Sato, Y. & Morishima, K. BlastKOALA and GhostKOALA: KEGG Tools for Functional Characterization of Genome and Metagenome Sequences. *J. Mol. Biol.* **428**, 726-731, doi:10.1016/j.jmb.2015.11.006 (2016).
34. Tatusova, T. *et al.* NCBI prokaryotic genome annotation pipeline. *Nucleic Acids Res.* **44**, 6614-6624, doi:10.1093/nar/gkw569 (2016).
35. Na, S. I. *et al.* UBCG: Up-to-date bacterial core gene set and pipeline for phylogenomic tree reconstruction. *J. Microbiol.* **56**, 280-285, doi:10.1007/s12275-018-8014-6 (2018).
36. Sasser, M. (MIDI technical note 101. Newark, DE: MIDI inc, 1990).
37. Collins, M. D. & Jones, D. A note on the separation of natural mixtures of bacterial ubiquinones using reverse-phase partition thin-layer chromatography and high performance liquid chromatography. *J. Appl. Bacteriol.* **51**, 129-134, doi:10.1111/j.1365-2672.1981.tb00916.x (1981).
38. Minnikin, D., Collins, M. & Goodfellow, M. Fatty acid and polar lipid composition in the classification of *Cellulomonas*, *Oerskovia* and related taxa. *J. Appl. Bacteriol.* **47**, 87-95, doi:10.1111/j.1365-2672.1979.tb01172.x (1979).
39. Trakunjae, C. *et al.* Enhanced polyhydroxybutyrate (PHB) production by newly isolated rare actinomycetes *Rhodococcus* sp. strain BSRT1-1 using response surface methodology. *Sci. Rep.* **11**, 1896, doi:10.1038/s41598-021-81386-2 (2021).
40. Juengert, J. R., Bresan, S. & Jendrossek, D. Determination of Polyhydroxybutyrate (PHB) Content in *Ralstonia eutropha* Using Gas Chromatography and Nile Red Staining. *Bio Protoc.* **8**, e2748, doi:10.21769/BioProtoc.2748 (2018).
41. Silva, L. F. *et al.* Poly-3-hydroxybutyrate (P3HB) production by bacteria from xylose, glucose and sugarcane bagasse hydrolysate. *J. Ind. Microbiol. Biotechnol.* **31**, 245-254, doi:10.1007/s10295-004-0136-7 (2004).
42. Thomas, T., Elain, A., Bazire, A. & Bruzard, S. Complete genome sequence of the halophilic PHA-producing bacterium *Halomonas* sp. SF2003: insights into its biotechnological potential. *World. J. Microbiol. Biotechnol.* **35**, 1-14, doi:10.1007/s11274-019-2627-8 (2019).
43. Neoh, S. Z. *et al.* Polyhydroxyalkanoate synthase (PhaC): The key enzyme for biopolyester synthesis. *Curr. Res. Biotechnol.* **4**, 87-101, doi:10.1016/j.crbiot.2022.01.002 (2022).
44. Luengo, J. M., Garcia, B., Sandoval, A., Naharro, G. & Olivera, E. R. Bioplastics from microorganisms. *Curr. Opin. Microbiol.* **6**, 251-260, doi:10.1016/s1369-5274(03)00040-7 (2003).
45. Sudesh, K., Abe, H. & Doi, Y. Synthesis, structure and properties of polyhydroxyalkanoates: biological polyesters. *Prog. Polym. Sci.* **25**, 1503-1555, doi:10.1016/S0079-6700(00)00035-6 (2000).
46. Rehm, B. H., Antonio, R. V., Spiekermann, P., Amara, A. A. & Steinbuchel, A. Molecular characterization of the poly(3-hydroxybutyrate) (PHB) synthase from *Ralstonia eutropha*: in vitro evolution, site-specific mutagenesis and development of a PHB synthase protein model. *Biochim Biophys Acta* **1594**, 178-190, doi:10.1016/s0167-4838(01)00299-0 (2002).
47. Yuan, W. *et al.* Class I and III polyhydroxyalkanoate synthases from *Ralstonia eutropha* and *Allochromatium vinosum*: characterization and substrate specificity studies. *Arch. Biochem. Biophys.*

- 394**, 87-98, doi:10.1006/abbi.2001.2522 (2001).
48. Rehm, B. H. Polyester synthases: natural catalysts for plastics. *Biochem. J.* **376**, 15-33, doi:10.1042/BJ20031254 (2003).
49. Mostafa, Y. S. *et al.* Bioplastic (poly-3-hydroxybutyrate) production by the marine bacterium *Pseudodonghicola xiamenensis* through date syrup valorization and structural assessment of the biopolymer. *Sci. Rep.* **10**, 1-13, doi:10.1038/s41598-020-65858-5 (2020).

## Figures

Fig. 1

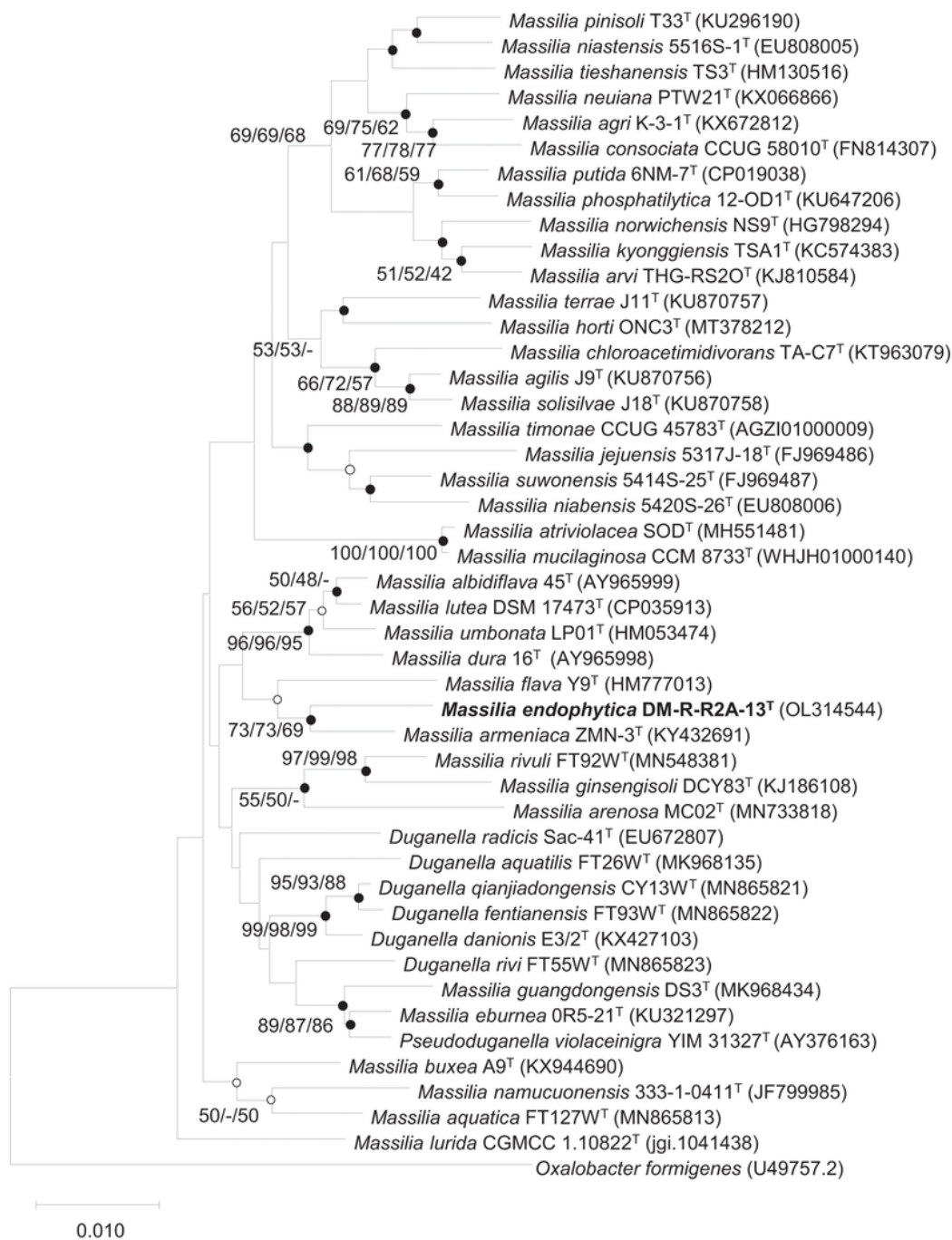


Figure 1

Phylogenetic tree of DM-R-R2A-13<sup>T</sup> and other members of the genus *Massilia* using neighbor-joining phylogenetic tree based on 16S rRNA gene sequences. Solid circles at the nodes indicate generic branches where the relationships were also established by ML and ME algorithms, while open circles indicate branches recovered by either ML or ME algorithms. Scale bar represents 0.010 substitutions per position.

Fig. 2

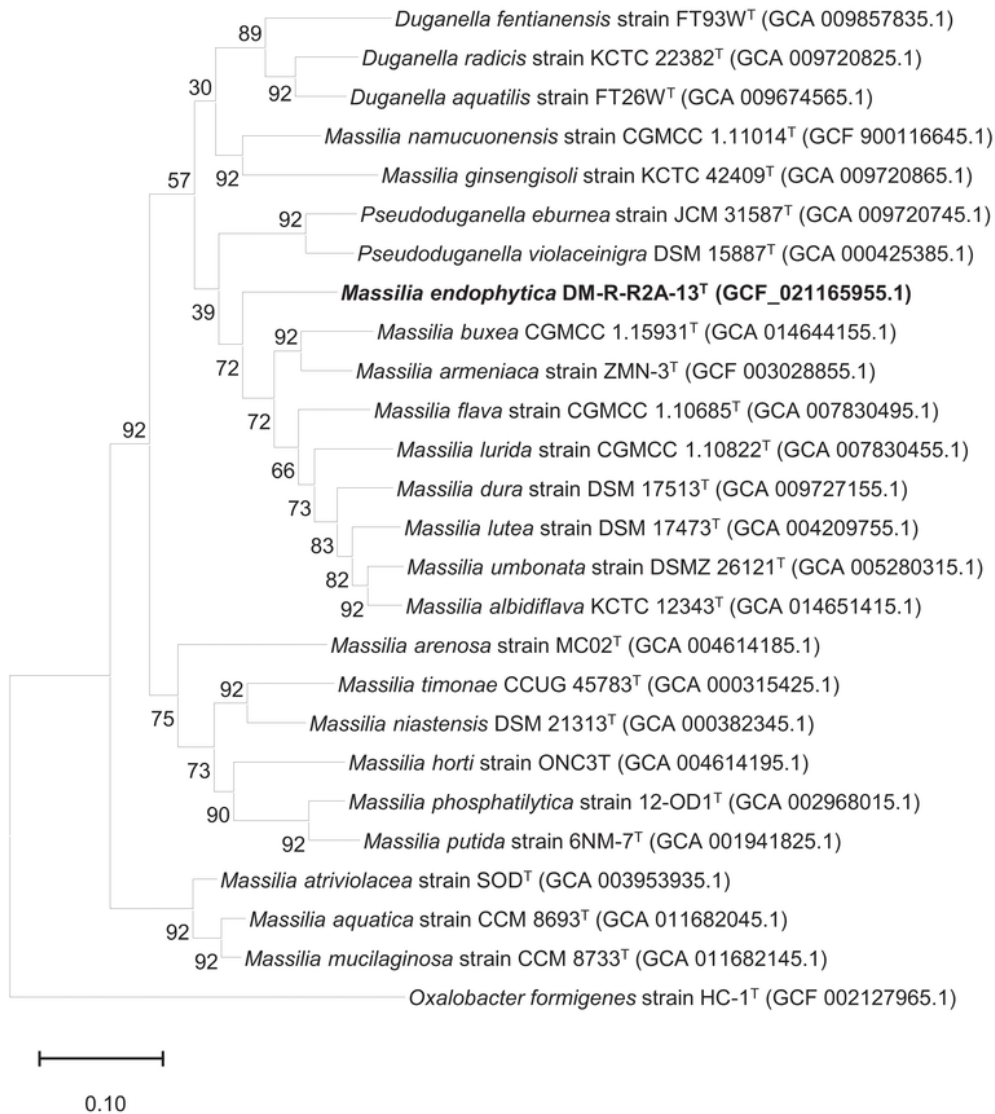
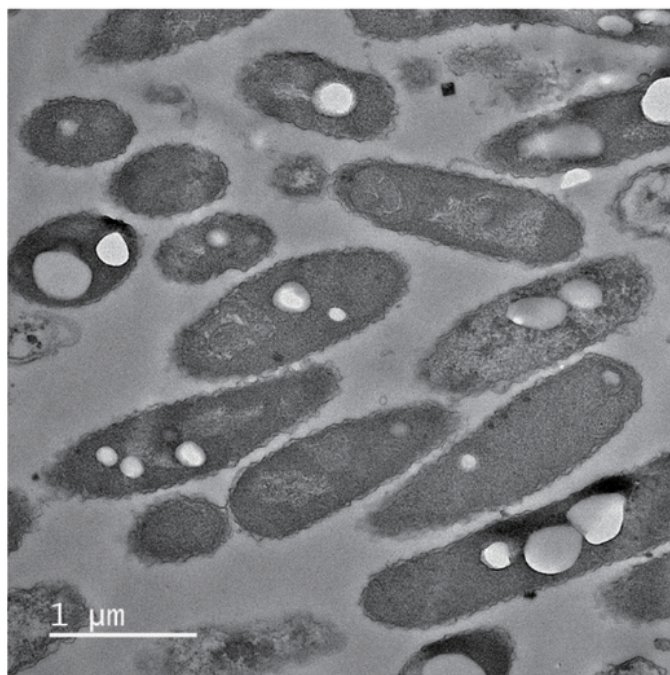


Figure 2

Phylogenomic tree of strain DM-R-R2A-13<sup>T</sup> based on the multiple alignments of 92 bacterial core gene sequences as determined by UBCG. Scale bar represents 0.020 substitutions per position.

**Fig. 3**



**Figure 3**

Transmission electron microscopy (TEM) image of strain DM-R-R2A-13<sup>T</sup> containing polyhydroxybutyrate (PHB) granules.

Fig. 4

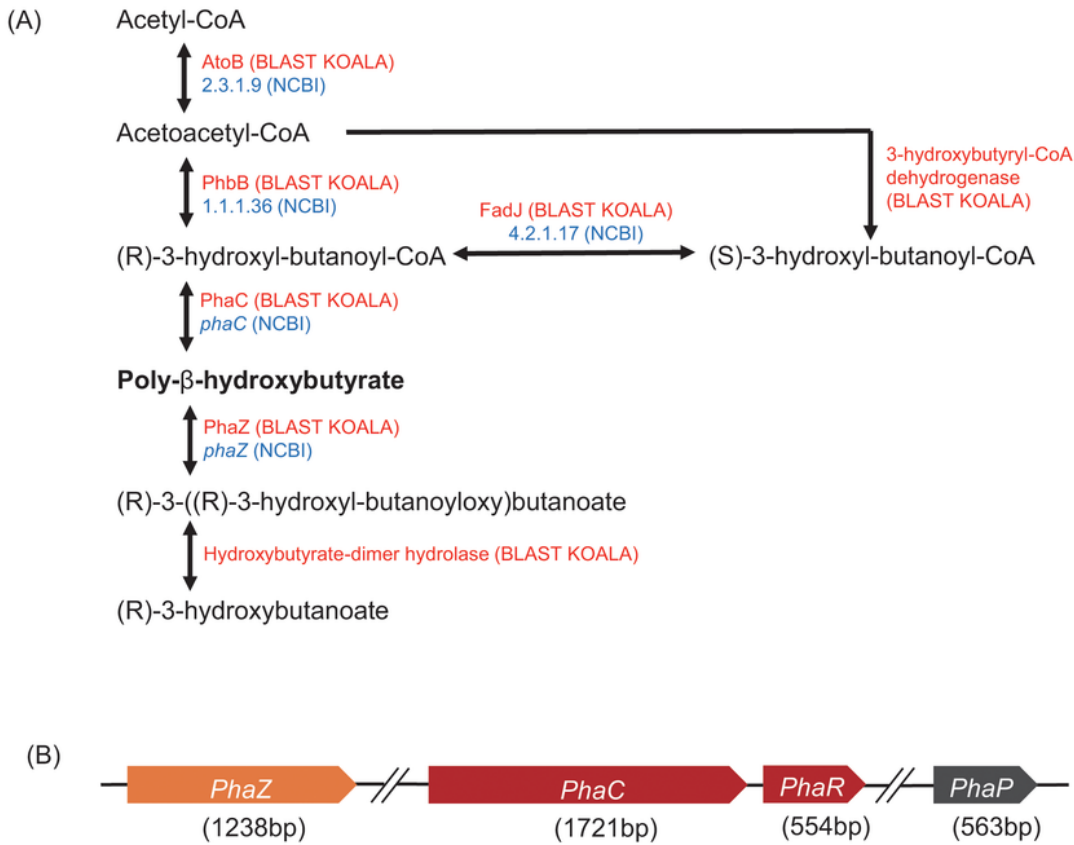


Figure 4

**Polyhydroxybutyrate (PHB) biosynthetic pathway and polyhydroxyalkanoate (PHA) synthase gene cluster in DM-R-R2A-13<sup>T</sup>.** (A) PHB biosynthetic pathway in strain DM-R-R2A-13<sup>T</sup>. AtoB, acetyl-CoA C-acetyltransferase; PhbB, Acetoacetyl-CoA reductase; PhaC, PHA synthase. Proteins identified in BlastKOALA analysis are marked in red with their names, and proteins identified in NCBI analysis are marked in blue with ID numbers. (B) PHA synthase gene cluster in strain DM-R-R2A-13<sup>T</sup>. phaC, class I

poly(R)-hydroxyalkanoic acid synthase; PhaR, PHA synthesis repressor; PhaP, TIGR01841 family phasin (small protein associated with inclusions such as PHA granules); PhaZ; PHA depolymerase.

Figure 5

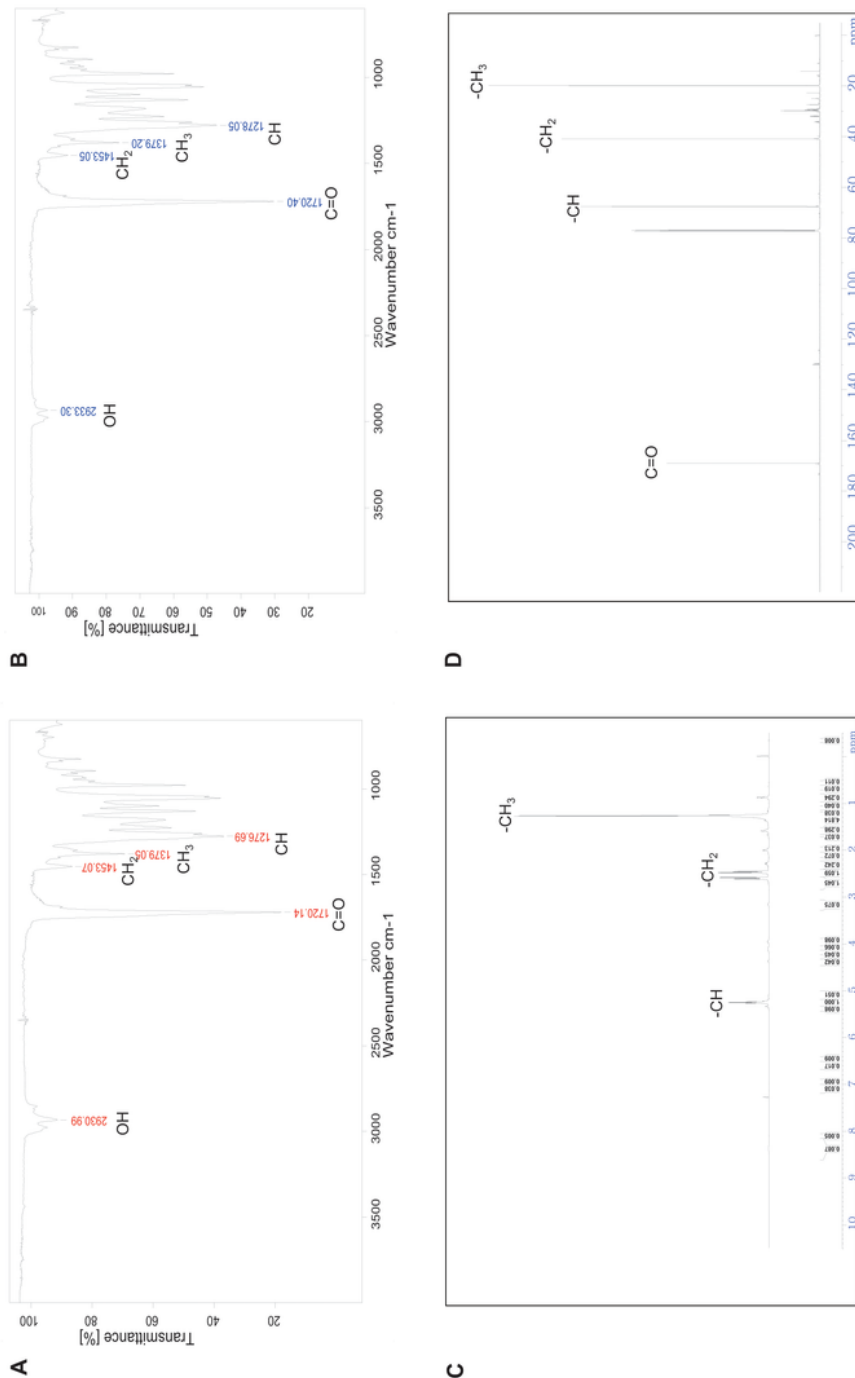
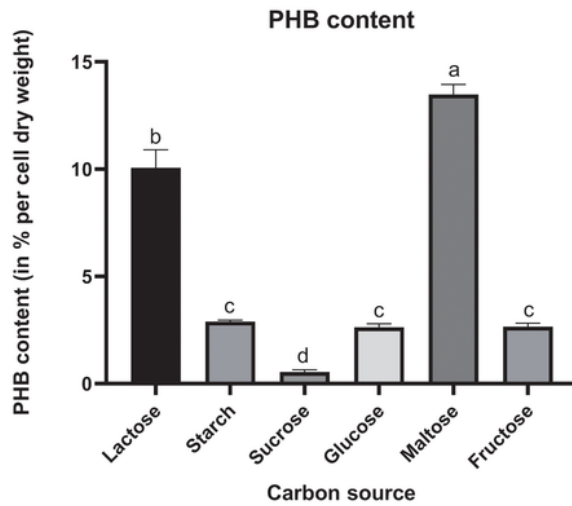


Figure 5

FT-IR and NMR spectra of PHB extracted from DM-R-R2A-13<sup>T</sup>. (A) FT-IR spectrum of PHB extracted from DM-R-R2A-13<sup>T</sup> showing absorption peaks at 2930.99, 1720.14, 1453.07, 1379.05, and 1276.69 cm<sup>-1</sup>,

corresponding to the OH, C=O, CH<sub>2</sub>, CH<sub>3</sub>, and CH groups, respectively. (B) FT-IR spectrum of commercial PHB (Sigma-Aldrich). (C) <sup>1</sup>H NMR spectrum has peaks at 1.26–1.28 ppm (-CH<sub>3</sub>), 2.45–2.62 ppm (-CH<sub>2</sub>), and 5.24–5.28 ppm (-CH). (D) <sup>13</sup>C NMR spectrum has peaks at 169.15, 67.61, 40.79, and 19.76 ppm, corresponding to the carbon atom of C=O, -CH, -CH<sub>2</sub>, and -CH<sub>3</sub>, respectively.

**Figure 6**



**Figure 6**



**Comparison of the effects of different carbon sources on PHB production by DM-R-R2A-13<sup>T</sup>.** Error bars indicate standard error (n=3). Means followed by different letters are significantly different at  $P < 0.05$  according to one-way ANOVA.

## Supplementary Files

This is a list of supplementary files associated with this preprint. Click to download.

- [SupplementarymaterialJeon.pdf](#)